NACA RM L56E30

NACA

RESEARCH MEMORANDUM

EXPLORATORY INVESTIGATION AT A MACH NUMBER OF 5.20 OF THE LONGITUDINAL AERODYNAMIC CHARACTERISTICS OF FLAT-BOTTOM BODIES

By Roy H. Lange

Langley Aeronautical Laboratory
Langley Field, Va.

NATIONAL ADVISORY COMMITTEE
FOR AERONAUTICS
WASHINGTON

July 27, 1956
Declassified July 11, 1961

NACA RM L56E30

NATIONAL ADVISORY COMMITTEE FOR AERONAUTICS

RESEARCH MEMORANDUM

EXPLORATORY INVESTIGATION AT A MACH NUMBER OF 5.20 OF THE LONGITUDINAL AERODYNAMIC CHARACTERISTICS OF FLAT-BOTTOM BODIES

By Roy H. Lange

SUMMARY

An exploratory investigation has been conducted at a Mach number of 5.20 to determine the longitudinal aerodynamic characteristics of a number of flat-bottom bodies which were investigated for possible hypersonic application. The bodies were tested at both positive and negative angles of attack to simulate flat-bottom and flat-top arrangements. Plan-form aspect ratios investigated ranged from 0.980 to 0.379, and the thicknesses of the bodies ranged from about 5 to 13 percent of the body length. Lift, drag, and pitching-moment data are presented herein and compared with predictions of shock-expansion theory for an angle-of-attack range sufficient to determine the maximum lift-drag ratio of each configuration. The Reynolds numbers ranged from about 2.42×10^6 to 3.75×10^6 based on body lengths of 7.75 inches and 12.00 inches, respectively.

INTRODUCTION

An interesting hypervelocity vehicle is the boost-glide missile. (See ref. 1.) Although investigations have been carried out at hypersonic speeds of a few body and wing-body configurations (see, for example, refs. 2 to 5), there is need for further research on this type of missile. The present report deals with the results of an exploratory investigation at a Mach number of 5.20 of the longitudinal aerodynamic characteristics of a number of simple body configurations of constant volume which may have application to the boost-glide missile. All configurations have one flat surface and were tested at both positive and negative angles of attack to simulate both flat-bottom and flat-top arrangements. The configurations investigated have triangular, half-elliptical, and trapezoidal plan forms. These plan forms were combined with triangular,

circular-arc, and trapezoidal cross sections. Plan-form aspect ratios investigated ranged from 0.980 to 0.379, and the thicknesses of the bodies ranged from about 5 to 13 percent of the body length. All bodies have blunt bases.

The investigation was conducted in the Langley gas dynamics laboratory at a Mach number of 5.20 and a test-section Reynolds number of 3.75×10^6 per foot. Lift, drag, and pitching-moment data are presented herein with a minimum of analysis.

SYMBOLS

α	angle of attack, deg
C_L	lift coefficient, Lift/qS
C_D	drag coefficient, Drag/qS
C_m	pitching-moment coefficient about nose of body, Pitching moment/qSl
x_{cp}/l	center-of-pressure location, body lengths from nose
L/D	lift-drag ratio
$(L/D)_{max}$	maximum lift-drag ratio
$C_{D_{min}}$	minimum drag coefficient
C_{D_f}	skin-friction drag coefficient
C_{L_α}	lift-curve slope, rate of change of lift coefficient with angle of attack, $\partial C_L/\partial\alpha$, per degree
q	free-stream dynamic pressure, $\rho V^2/2$
S	plan-form area
S_b	base area
R_l	Reynolds number based on body length

l	length of model
A	plan-form aspect ratio, b^2/S
b	model span
M	Mach number, V/a
V	free-stream velocity
ρ	mass density of air
a	velocity of sound in air
t	body thickness at base

MODELS

The geometric characteristics of the bodies tested are given in figure 1. All bodies have the same volume. Bodies 1, 2, and 5 have simple triangular plan forms with triangular cross sections having widths of three times the height for body 1, five times the height for body 2, and 2.25 times the height for body 5. Body 3 is the same as body 2 for a distance of 6.667 inches from the nose; after this point a constant-area section is added. Body 4 is formed by the intersection of an inclined plane with the surface of a cylinder of 3.020-inch radius. The plane is inclined 4.76° to the axis of the cylinder. Body 6 has a composite sweep plan form designed to approximate the plan form of body 4. Bodies 7 and 9 have 5°-wedge center sections with triangular edges swept approximately at the Mach lines for the test Mach number of 5.20. Body 8 is the same as body 7 for a distance of 6 inches from the nose; after this point a constant-area section is added.

The models were constructed of Fiberglas and heat-resistant Paraplex and had very smooth finishes which did not deteriorate after repeated tests in the wind tunnel. The leading edges of the bodies had a thickness of about 0.012 inch. No noticeable deflections of the component parts of the models under load (maximum normal-force limit of strain-gage balance = 6 pounds) were noted during the tests.

Except for bodies 8 and 9, a 1/2-inch-diameter hole was drilled in and perpendicular to the base of each body for the purpose of mounting each body on the 1/2-inch-diameter sting attached to the externally mounted strain-gage balance. The body and sting were held together with set screws. The base of each body was about 1 inch upstream of the leading edge of a wedge-shaped shield (total angle, 20°) which housed the

strain-gage balance. For bodies 8 and 9, which were too thin at the base for a 1/2-inch-diameter hole, a 1/4-inch by 1/2-inch sting having an adapter with a 1/2-inch hole at the end was attached at the base. The distance from the base of the body to the adapter was 1.75 inches. A 1/8-inch-diameter tube attached to the balance housing was made to project to within 1/16 inch of the base of each body for the measurement of the base pressure.

APPARATUS AND TESTS

The tests were conducted in a Langley gas dynamics jet which is of the intermittent type with a high-pressure reservoir and a vacuum sphere having a capacity of 36,000 cubic feet. A heat exchanger is used to heat the air to the desired stagnation temperature. The two-dimensional nozzle has a rectangular test section approximately 12 inches high and 9 inches wide. The nozzle was designed by the method of characteristics, with a correction made for boundary layer, and operates at an average Mach number of 5.20. A variable-area supersonic diffuser is provided, and the running time of the tests varied from about 6 minutes to a maximum of about 10 minutes, depending upon the model configuration and the angle-of-attack range. All tests were made at a stagnation pressure of 100-pounds-per-square-inch gage. A stagnation temperature of 250° F was maintained to avoid the possibility of liquefaction of the air in the test section. The Reynolds number of the tests was about 3.75×10^6 per foot.

The angle-of-attack range of the tests was from about -6° to 10° and was limited by the strain-gage-balance maximum normal force of ±6 pounds. The tests were made at positive angles of attack to simulate flat-bottom arrangements and at negative angles of attack to simulate flat-top arrangements. At each angle of attack, measurements were made of the normal force, chord force, and pitching moment by means of a sting-supported external electrical strain-gage balance. The balance and model rotated on the angle-of-attack mechanism. The maximum design conditions for the balance are ±6 pounds of normal force, ±10 inch-pounds of pitching moment, and 1 pound of chord force. The base pressure was measured throughout the angle-of-attack range for each model. The angles of attack were determined from schlieren photographs of the models at each attitude and are accurate to ±0.1°.

The base pressures measured were used to calculate the chord force acting at the base of the bodies and the chord forces measured by the strain-gage balance were corrected to the condition of free-stream static pressure acting at the base.

PRESENTATION OF DATA

The results of the investigation are presented in table I and figures 2 to 10, and schlieren photographs of four of the body shapes are presented in figure 11 at angles of attack for maximum lift-drag ratio. For each body in figures 2 to 10 the variations of α, C_D, L/D, C_m, and x_{cp}/l with lift coefficient C_L are presented. Also presented in figures 2 to 10 for comparison purposes are the predictions of two-dimensional shock-expansion theory plus turbulent boundary-layer skin friction for the lift curve, the drag polar, and the variation of L/D with C_L.

The forces acting on the bodies were calculated by the use of shock-expansion theory. Conical-flow regions were ignored. The pressures acting on the upper surface of the bodies with triangular plan forms were determined by the angle that the inclined plane on the upper surface made with the relative wind - the ridge angle was not used. For body 4 the pressure was considered constant on the upper surface and was determined by the wedge angle along the plane of symmetry.

An effective Reynolds number was determined for each body in order that the skin-friction drag could be estimated by use of the method of Van Driest (ref. 6). For the triangular plan-form bodies the results of reference 7 were used where it was found for laminar boundary layers that a length equal to 9/16 the length of the root chord of a triangular wing gives the average skin-friction coefficient. By similar reasoning, for turbulent boundary layers a length equal to 0.59 the length of the root chord was used (for which the skin friction varies inversely as the 1/4 to 1/5 power of the Reynolds number). For body 3, 9/16 of the root chord of the triangular portion of the plan form plus the length of the rectangular portion was used, and for body 8 the average chord of the front portion plus the length of the rectangular portion was used. The average chord S/b was used for bodies 4, 6, 7, and 9. The lift and drag coefficients were computed by using both laminar and turbulent values of skin-friction coefficients; however, only the turbulent values are plotted on the figures since it was found that the drag coefficients including laminar boundary-layer skin friction were much lower than the experimental values.

SUMMARY OF RESULTS

No detailed discussion of the results of the investigation is attempted in this paper; however, the results of most interest are pointed out in this section.

The force-test results are summarized in the following table:

Model body	Thickness, t/l	R_l	C_{L_α} ($C_L = 0$)	$C_{D_{min}}$	$(L/D)_{max}$	$(L/D)_{max}$ for model inverted
1	0.127	3.12×10^6	0.0141	0.0084	5.45	4.66
2	.098	3.12	.0156	.0077	5.50	5.00
3	.055	3.73	.0129	.0053	5.85	----
4	.083	3.12	.0130	.0058	6.14	5.34
5	.111	3.75	.0121	.0069	5.50	4.65
6	.071	3.09	.0128	.0058	6.07	5.14
7	.088	2.86	.0156	.0066	5.80	5.50
8	.052	3.16	.0126	.0046	6.30	6.40
9	.088	2.42	.0141	.0061	6.30	6.00

The triangular plan-form bodies (bodies 1, 2, and 5) with the highest values of thickness ratio have the highest values of $C_{D_{min}}$ and, consequently, the lowest value of $(L/D)_{max}$. The lift-curve slope of body 2, however, is equal to the highest value obtained in the tests. It should be noted that the thickness, length, Reynolds number, and plan form are all variable, and the changes in aerodynamic characteristics result from all these variations.

The maximum lift-drag ratio is, of course, influenced by the nature of the boundary layer. Since there was some evidence of transition near the nose of the bodies in the schlieren photographs, and since the theoretical results assuming turbulent boundary layers agreed with the experiments, and since the addition of transition strips had no effect, it may be assumed that the boundary layer was largely turbulent.

Reducing the thickness ratio by incorporating a rectangular section in the plan form reduces $C_{D_{min}}$ but, at the same time, reduces C_{L_α}. However, the overall effect is to increase $(L/D)_{max}$. (Compare bodies 2 and 3 and bodies 7 and 8.) Some of the increase in $(L/D)_{max}$ may result from the increase in Reynolds number R_l for bodies 3 and 8.

All bodies with the exception of body 8 have higher values of $(L/D)_{max}$ as flat-bottom bodies than as flat-top bodies; however, for bodies 7, 8, and 9, the differences in $(L/D)_{max}$ are small.

All bodies have a linear variation of pitching-moment coefficient about the nose with lift coefficient throughout the range of lift coefficients investigated. The changes in center-of-pressure location are generally small throughout the lift-coefficient range (except for points

near $C_L = 0$), with the largest variations being measured for bodies which have a change in slope of the upper surface in the streamwise direction.

Langley Aeronautical Laboratory,
National Advisory Committee for Aeronautics,
Langley Field, Va., May 8, 1956.

REFERENCES

1. Steiff, Alvin, and Allen, H. Julian: Some Aspects of the Design of Hypersonic Boost-Glide Aircraft. NACA RM A55E26, 1955.

2. Ridyard, Herbert W.: The Aerodynamic Characteristics of Two Series of Lifting Bodies at Mach Number 6.86. NACA RM L54C15, 1954.

3. Resnikoff, Meyer M.: Optimum Lifting Bodies at High Supersonic Airspeeds. NACA RM A54B15, 1954.

4. Eggers, A. J., Jr., and Syvertson, Clarence A.: Aircraft Configurations Developing High Lift-Drag Ratios at High Supersonic Speeds. NACA RM A55L05, 1956.

5. McLellan, Charles H., and Dunning, Robert W.: Factors Affecting the Maximum Lift-Drag Ratio at High Supersonic Speeds. NACA RM L55L20a, 1956.

6. Van Driest, E. R.: Turbulent Boundary Layer in Compressible Fluids. Jour. Aero. Sci., vol. 18, no. 3, Mar. 1951, pp. 145-160, 216.

7. Bertram, Mitchel H., and McCauley, William D.: An Investigation of the Aerodynamic Characteristics of Thin Delta Wings With a Symmetrical Double-Wedge Section at a Mach Number of 6.9. NACA RM L55B14, 1955.

TABLE I.- LONGITUDINAL CHARACTERISTICS OF BODIES

TESTED AT A MACH NUMBER OF 5.20.

Model	α, deg	C_L	C_D	C_m	L/D
Body 1	-3.20	-0.0884	0.0204	0.0583	-4.34
	-2.00	- .0723	.0156	.0474	-4.65
	- .90	- .0568	.0127	.0373	-4.472
	2.72	- .0103	.0086	.0057	-1.19
	3.60	.0036	.0084	-.0036	.43
	5.08	.0235	.0090	-.0170	2.61
	6.20	.0407	.0098	-.0286	4.15
	7.33	.0594	.0116	-.0411	5.12
	8.37	.0768	.0142	-.0529	5.41
Body 2	-1.03	- .0544	.0116	.0363	-4.69
	-1.00	- .0566	.0111	.0376	-5.11
	0	- .0399	.0093	.0265	-4.32
	1.35	- .0213	.0080	.0144	-2.67
	3.00	.0041	.0077	-.0026	.53
	4.20	.0261	.0082	-.0170	3.18
	4.37	.0252	.0086	-.0164	2.93
	5.45	.0480	.0100	-.0316	4.80
	5.82	.0489	.0096	-.0320	5.08
	7.25	.0721	.0132	-.0476	5.47
	7.82	.0824	.0157	-.0545	5.25
Body 3	1.77	.0087	.0053	-.0106	1.62
	2.85	.0199	.0059	-.0169	3.37
	4.18	.0319	.0068	-.0232	4.68
	5.50	.0547	.0094	-.0377	5.80
	6.95	.0741	.0128	-.0495	5.79
Body 4	-2.92	-.0671	.0126	.0394	-5.33
	-1.92	-.0497	.0095	.0288	-5.21
	- .80	-.0351	.0076	.0202	-4.62
	.47	-.0203	.0064	.0115	-3.18
	1.75	-.0046	.0059	.0023	- .78
	2.75	.0101	.0059	-.0062	1.71
	4.18	.0254	.0065	-.0151	3.94
	5.08	.0436	.0078	-.0257	5.59
	6.55	.0629	.0103	-.0365	6.13
Body 5	- 6.03	-.0968	.0243	.0652	-3.98
	- 5.12	-.0836	.0201	.0557	-4.16
	- 3.88	-.0721	.0155	.0467	-4.65
	- 2.70	-.0587	.0129	.0383	-4.54
	- 1.62	-.0453	.0104	.0292	-4.37
	- .62	-.0325	.0086	.0211	-3.76
	1.47	-.0099	.0071	.0051	-1.42
	2.68	.0020	.0069	-.0029	.29
	3.98	.0188	.0074	-.0142	2.55
	5.17	.0323	.0081	-.0228	4.01
	6.34	.0472	.0094	-.0329	5.01
	7.43	.0627	.0115	-.0437	5.47
	8.52	.0782	.0143	-.0543	5.46
	9.73	.0954	.0184	-.0662	5.18
	10.78	.1141	.0235	-.0791	4.86
Body 6	- 3.73	-.0661	.0130	.0309	-5.09
	- 3.23	-.0565	.0110	.0258	-5.14
	- 2.08	-.0405	.0085	.0174	-4.77
	- .78	-.0227	.0066	.0082	-3.44
	.33	-.0071	.0059	.0001	-1.20
	1.55	.0082	.0058	-.0077	1.41
	2.90	.0240	.0063	-.0158	3.81
	4.22	.0418	.0077	-.0253	5.43
	5.23	.0588	.0097	-.0342	6.06
	6.00	.0680	.0113	-.0392	6.02
Body 7	-2.62	-.0685	.0125	.0403	-5.48
	-1.48	-.0529	.0098	.0309	-5.40
	- .37	-.0389	.0081	.0224	-4.80
	.73	-.0232	.0072	.0128	-3.22
	2.00	-.0076	.0067	.0035	-1.13
	2.93	.0091	.0067	-.0066	1.36
	4.17	.0257	.0074	-.0166	3.47
	5.00	.0425	.0085	-.0267	5.00
	6.35	.0609	.0108	-.0377	5.64
	6.83	.0704	.0121	-.0435	5.82
	7.73	.0788	.0139	-.0486	5.67
Body 8	-3.17	-.0551	.0087	.0274	-6.33
	-2.57	-.0477	.0075	.0230	-6.36
	-1.93	-.0400	.0066	.0188	-6.06
	- .68	-.0241	.0054	.0098	-4.46
	.50	-.0084	.0046	.0012	-1.83
	1.80	.0067	.0047	-.0073	1.43
	3.07	.0216	.0057	-.0152	3.79
	4.21	.0376	.0068	-.0246	5.53
	5.53	.0557	.0090	-.0346	6.19
	6.18	.0658	.0106	-.0402	6.12
Body 9	-2.42	-.0799	.0132	.0498	-6.05
	-1.13	-.0466	.0092	.0255	-5.07
	.03	-.0282	.0075	.0147	-3.76
	1.22	-.0087	.0064	.0032	-1.36
	3.00	.0110	.0061	-.0080	1.80
	4.22	.0315	.0070	-.0199	4.50
	5.50	.0530	.0089	-.0327	5.96
	6.85	.0744	.0118	-.0451	6.31

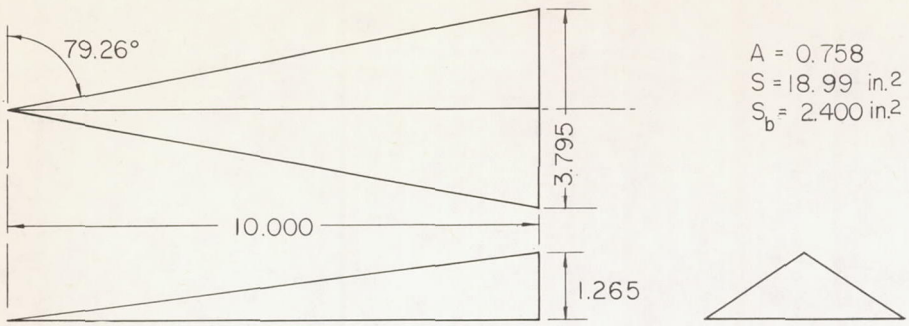

(a) Body 1.

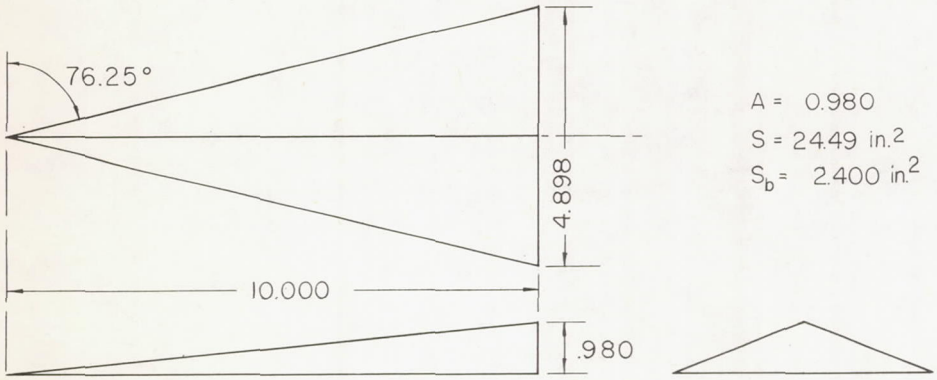

(b) Body 2.

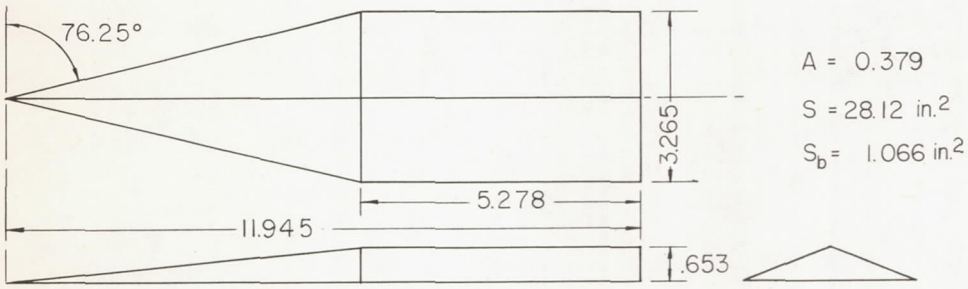

(c) Body 3.

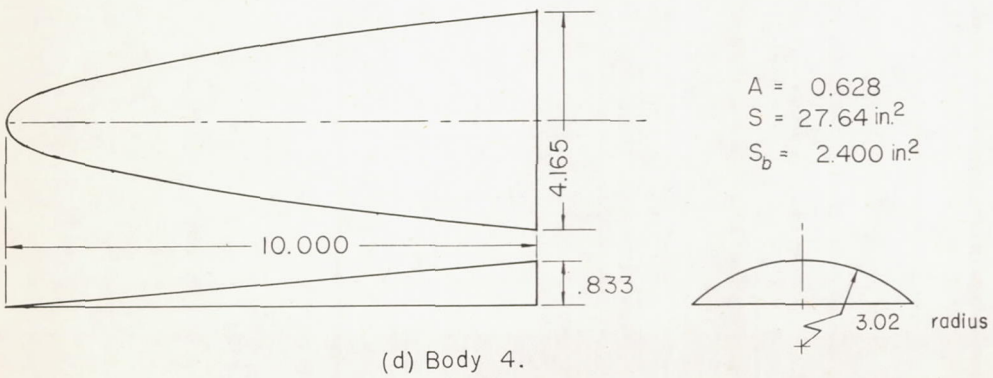

(d) Body 4.

Figure 1.- Geometric characteristics of bodies investigated at M = 5.20. All dimensions are in inches except where noted.

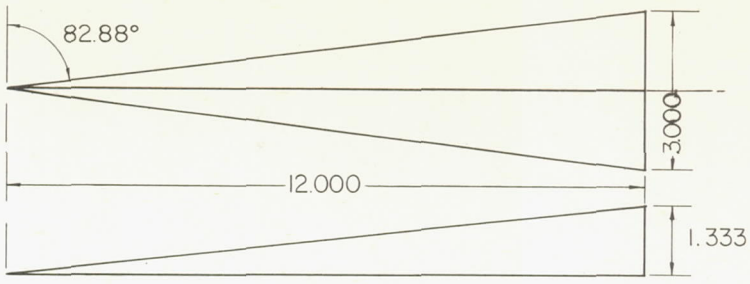

A = 0.500
S = 18.00 in.^{2}
S_b = 2.000 in.^{2}

(e) Body 5.

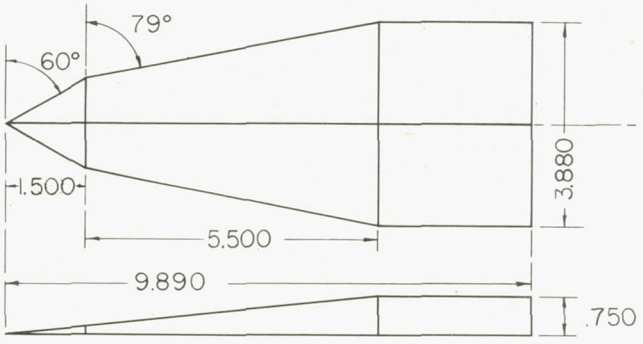

A = 0.538
S = 27.95 in.^{2}
S_b = 1.273 in.^{2}

(f) Body 6.

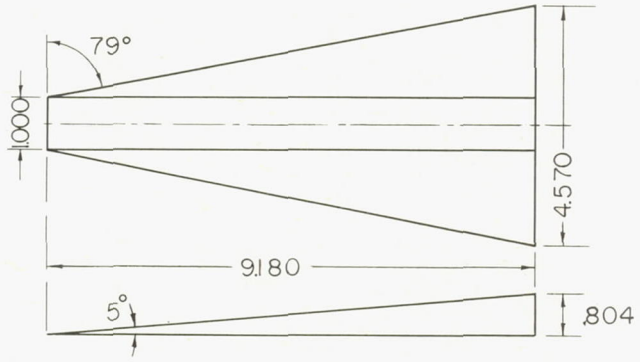

A = 0.817
S = 25.56 in.^{2}
S_b = 2.239 in.^{2}

(g) Body 7.

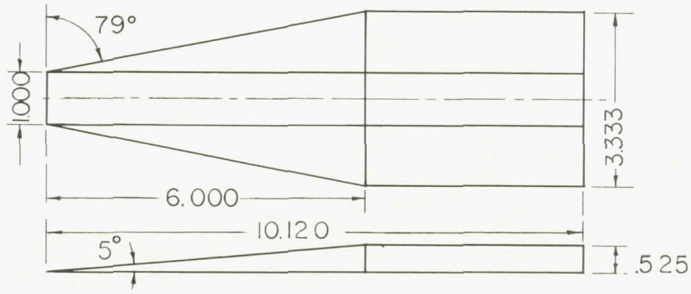

A = 0.423
S = 26.24 in.^{2}
S_b = 1.137 in.^{2}

(h) Body 8.

Figure 1.- Continued.

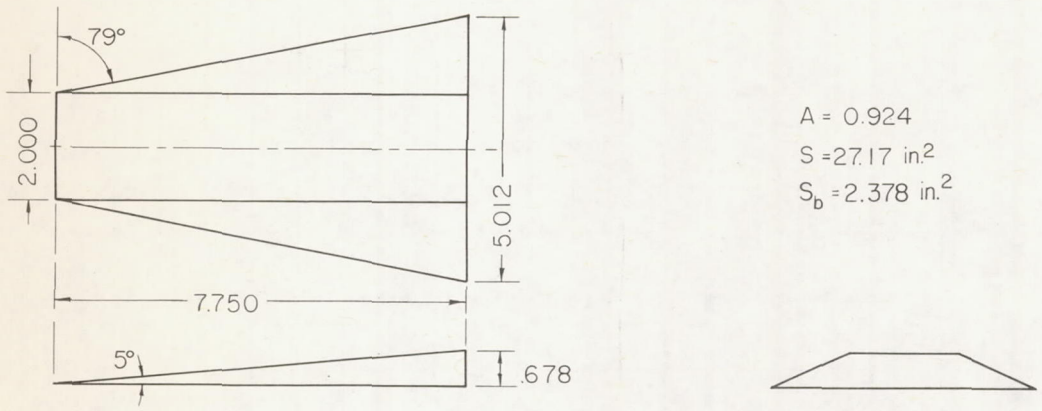

(i) Body 9.

Figure 1.- Concluded.

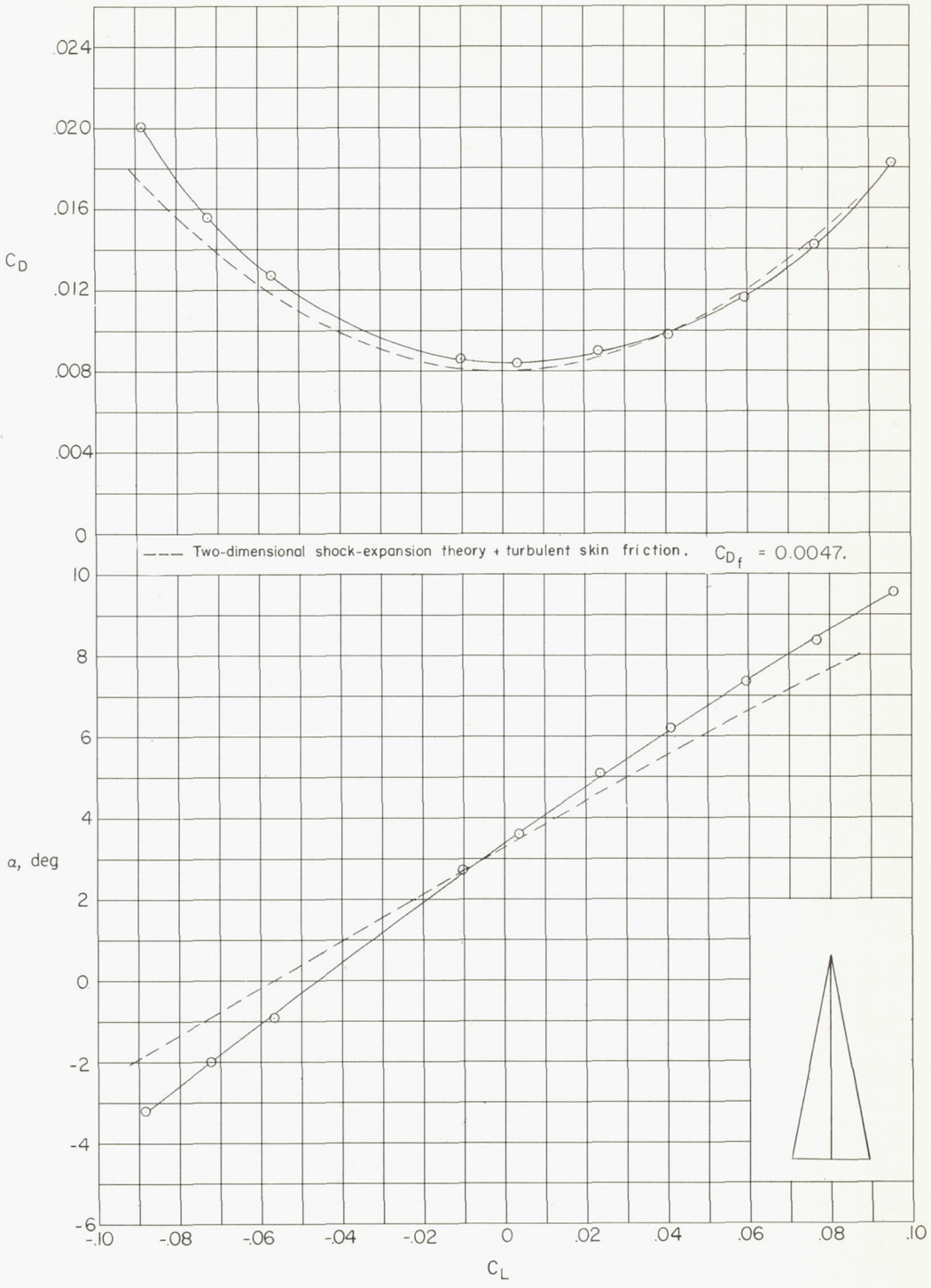

Figure 2.- Longitudinal aerodynamic characteristics of body 1 at M = 5.20.

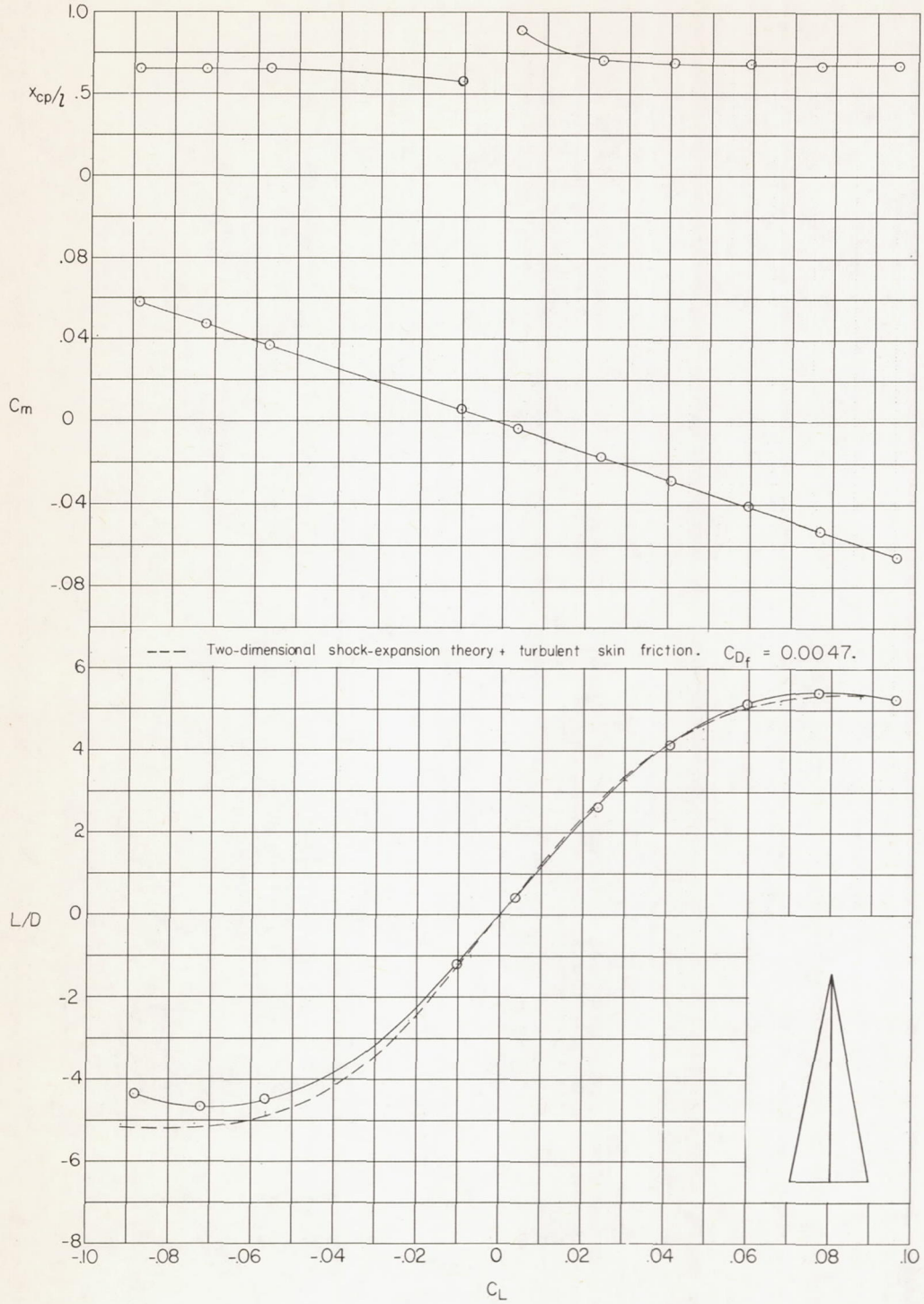

Figure 2.- Concluded.

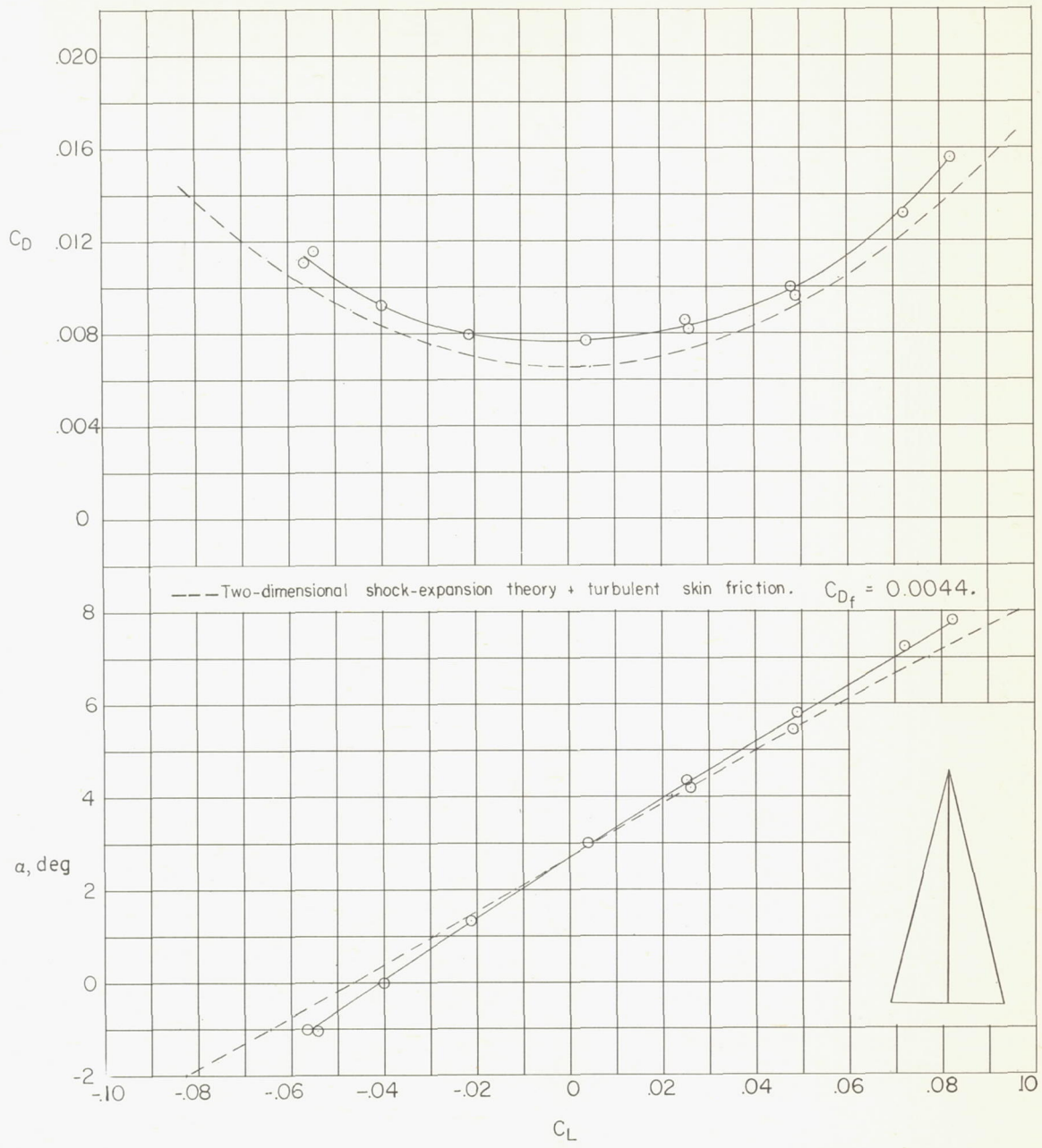

Figure 3.- Longitudinal aerodynamic characteristics of body 2 at M = 5.20.

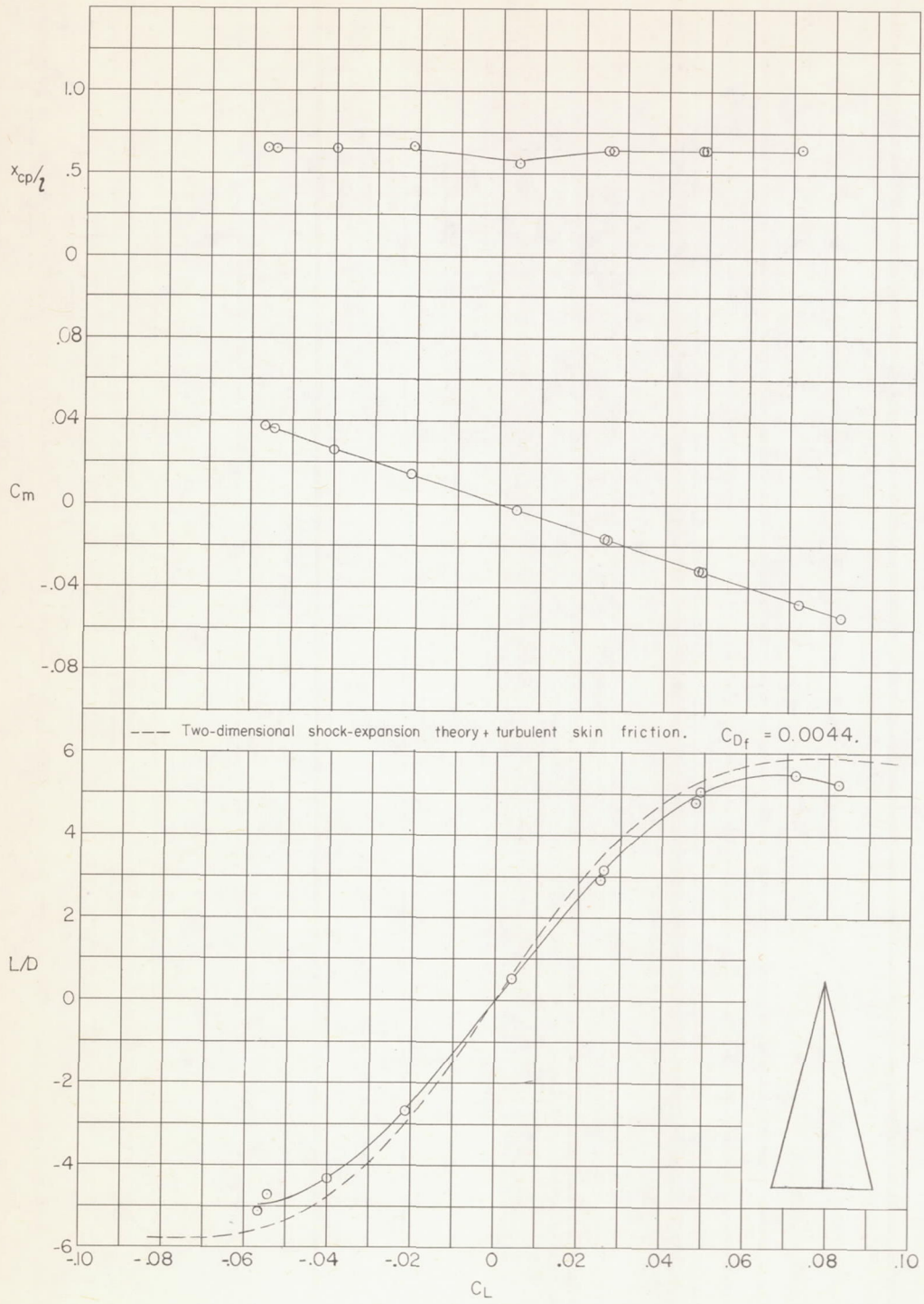

Figure 3.- Concluded.

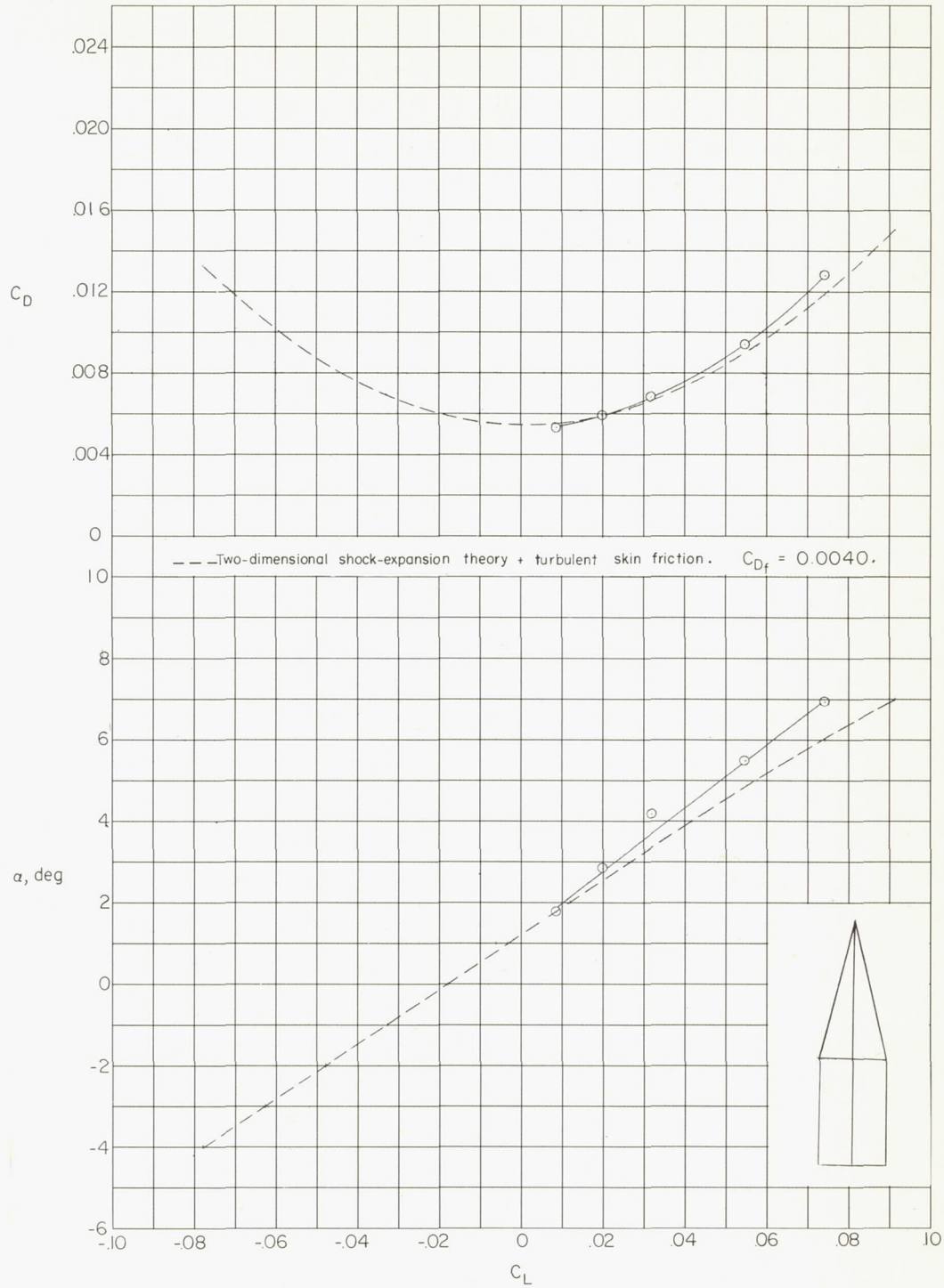

Figure 4.- Longitudinal aerodynamic characteristics of body 3 at M = 5.20.

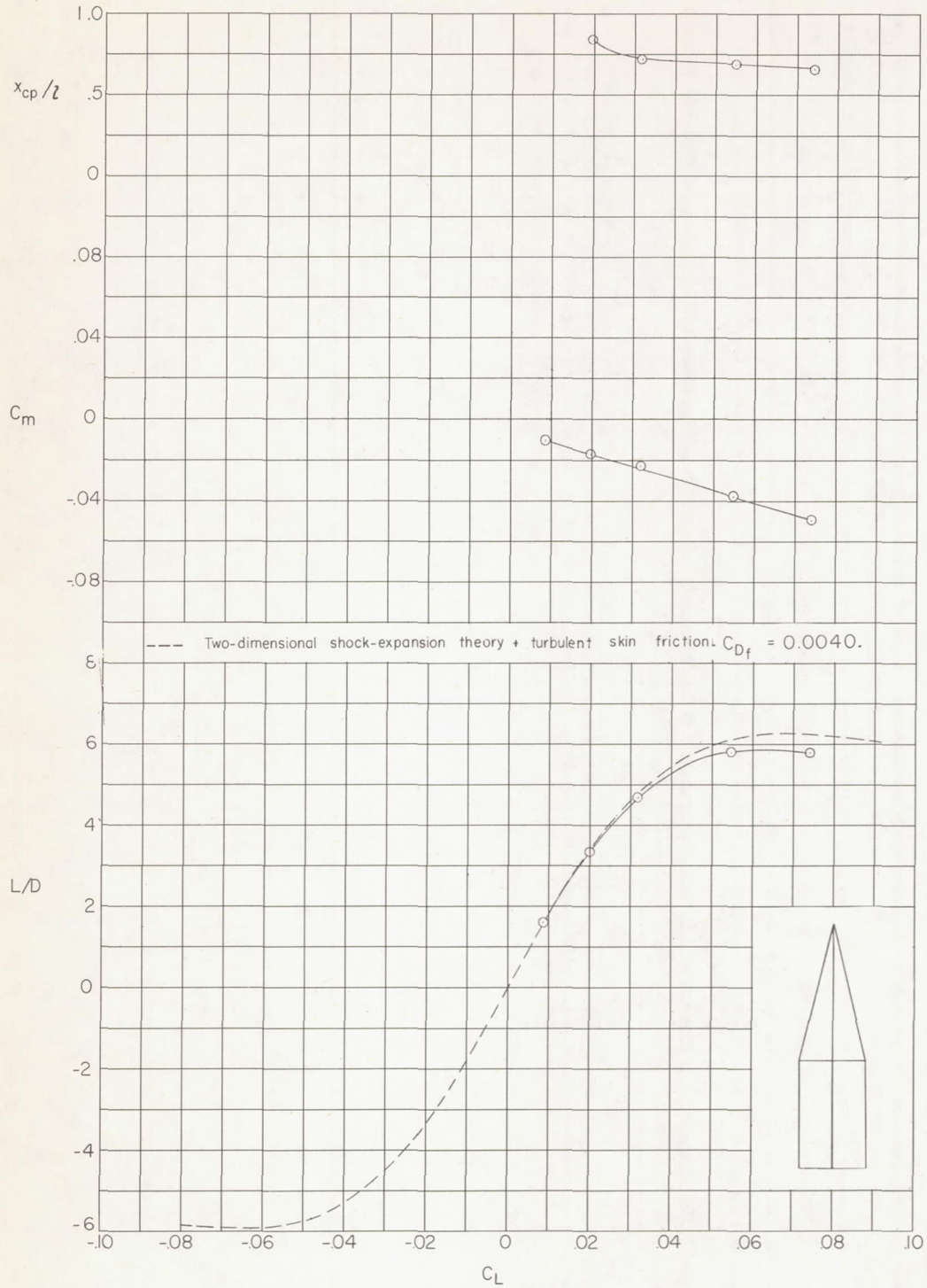

Figure 4.- Concluded.

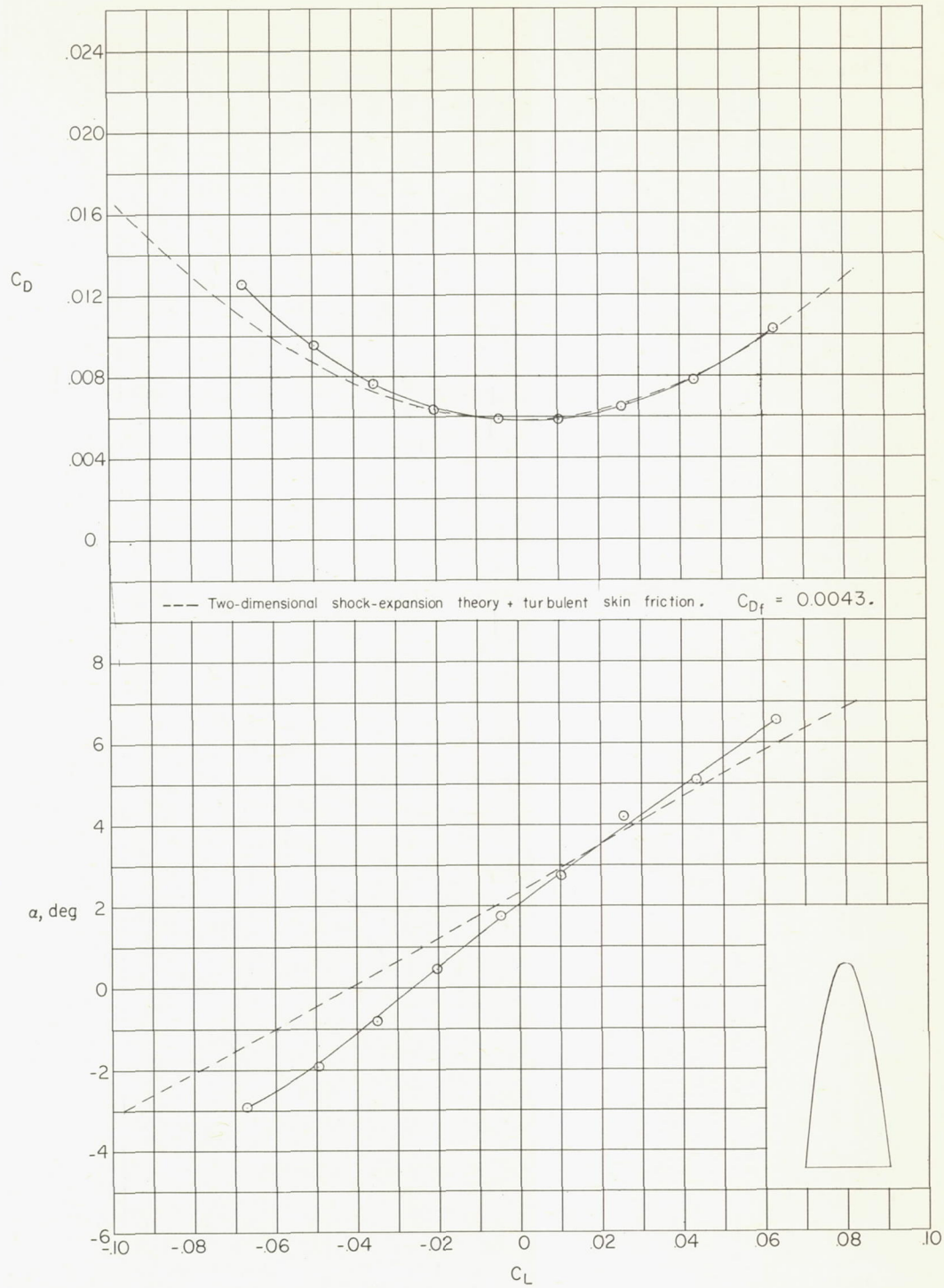

Figure 5.- Longitudinal aerodynamic characteristics of body 4 at M = 5.20.

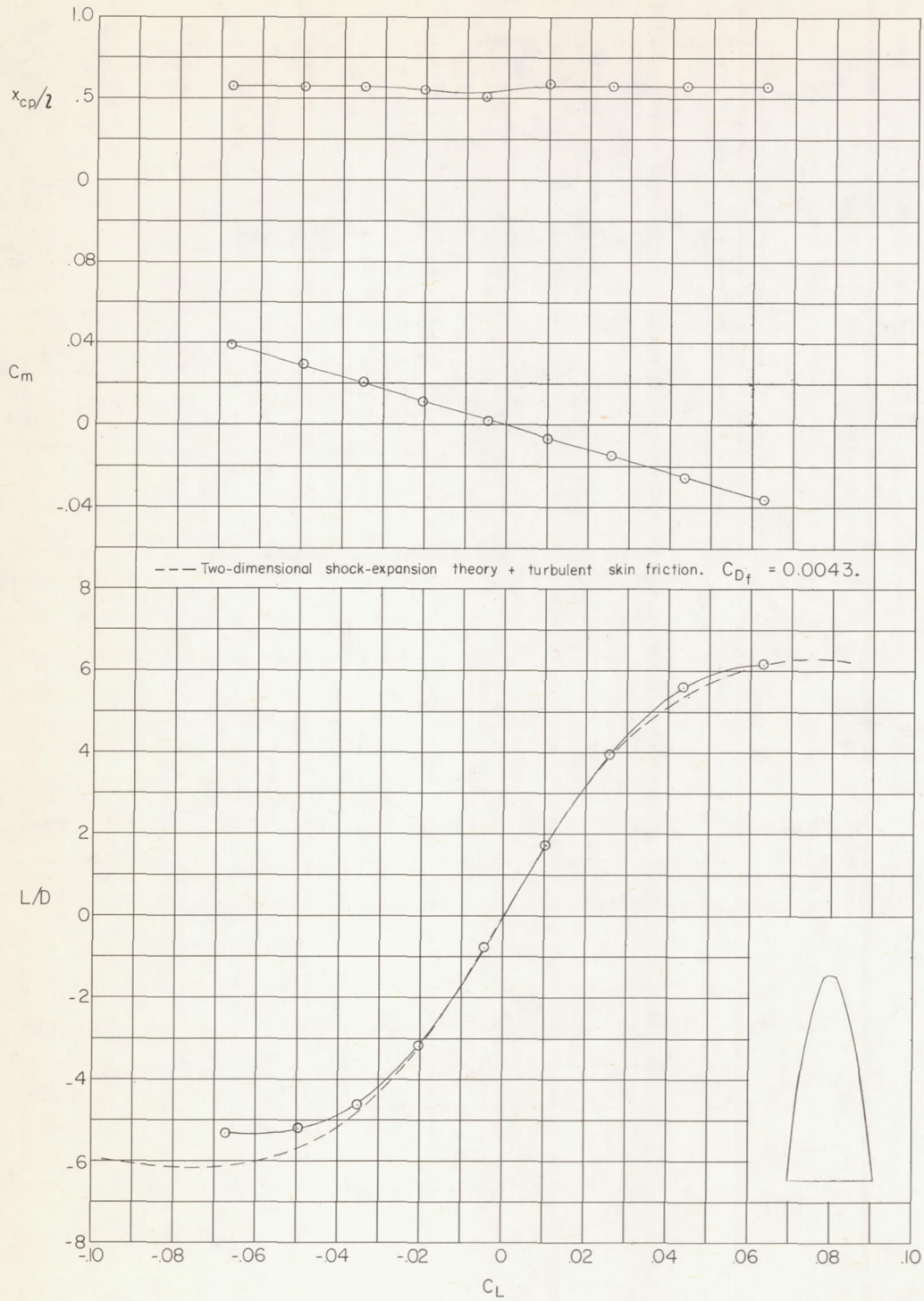

Figure 5.- Concluded.

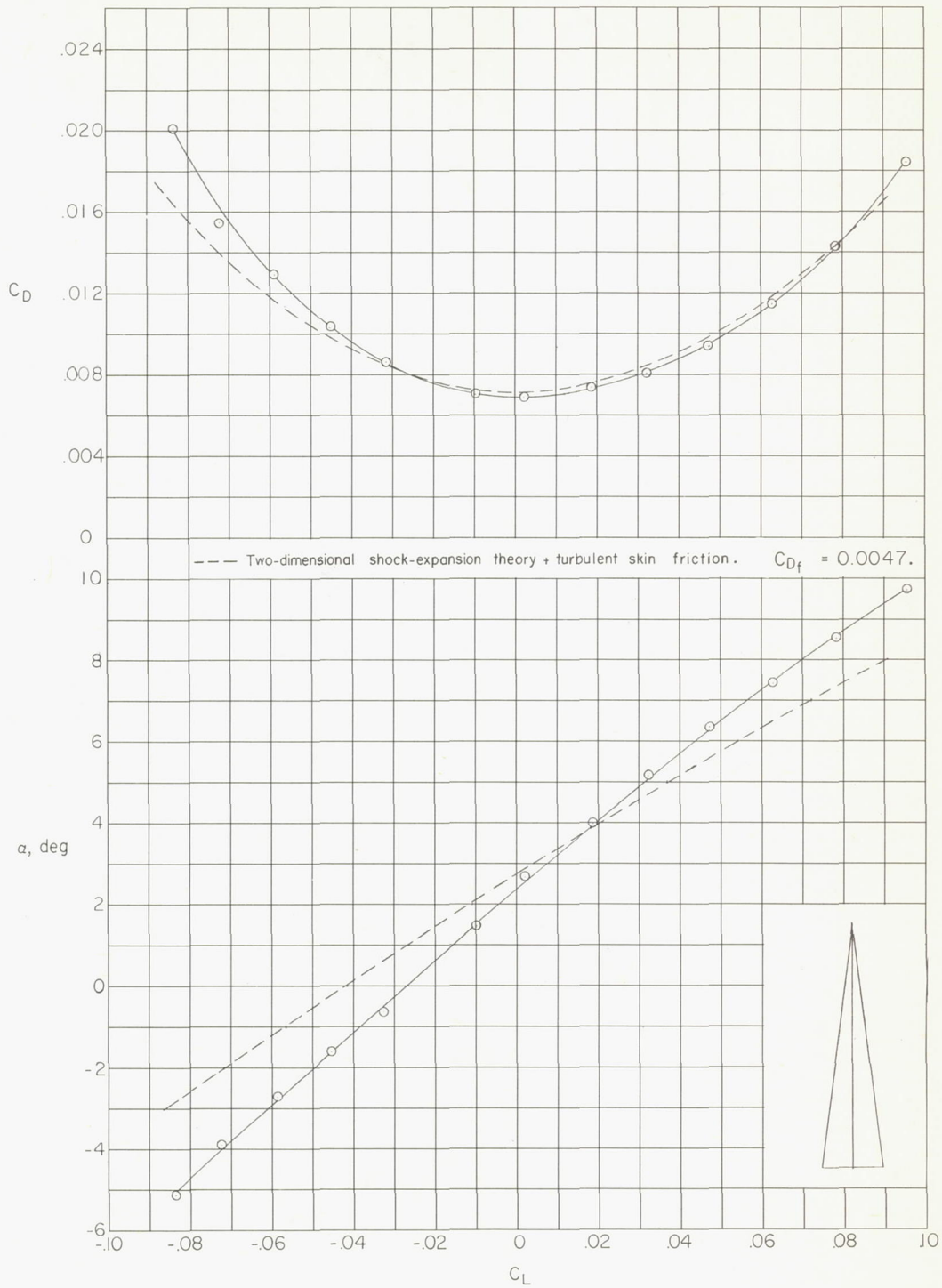

Figure 6.- Longitudinal aerodynamic characteristics of body 5 at M = 5.20.

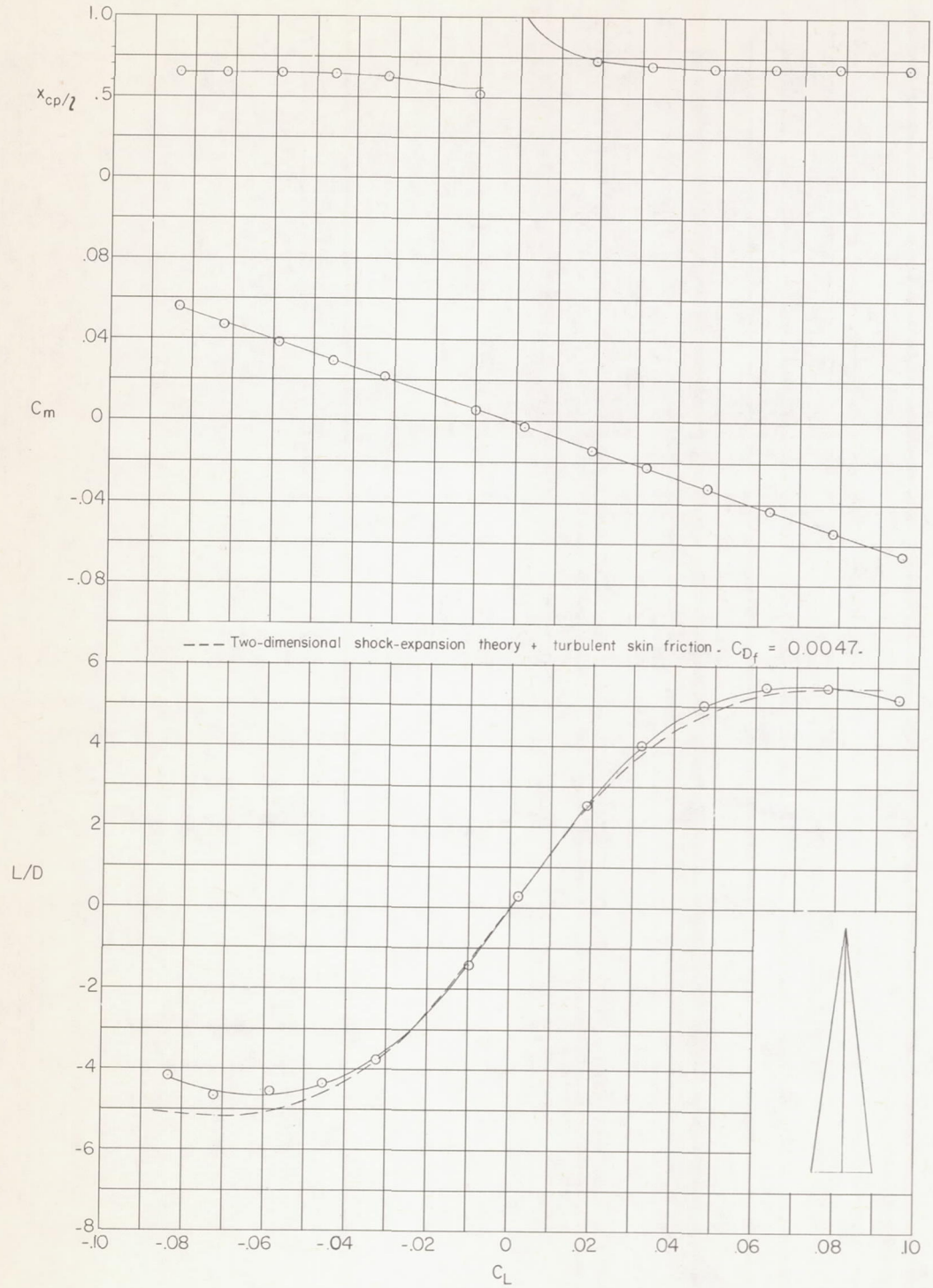

Figure 6.- Concluded.

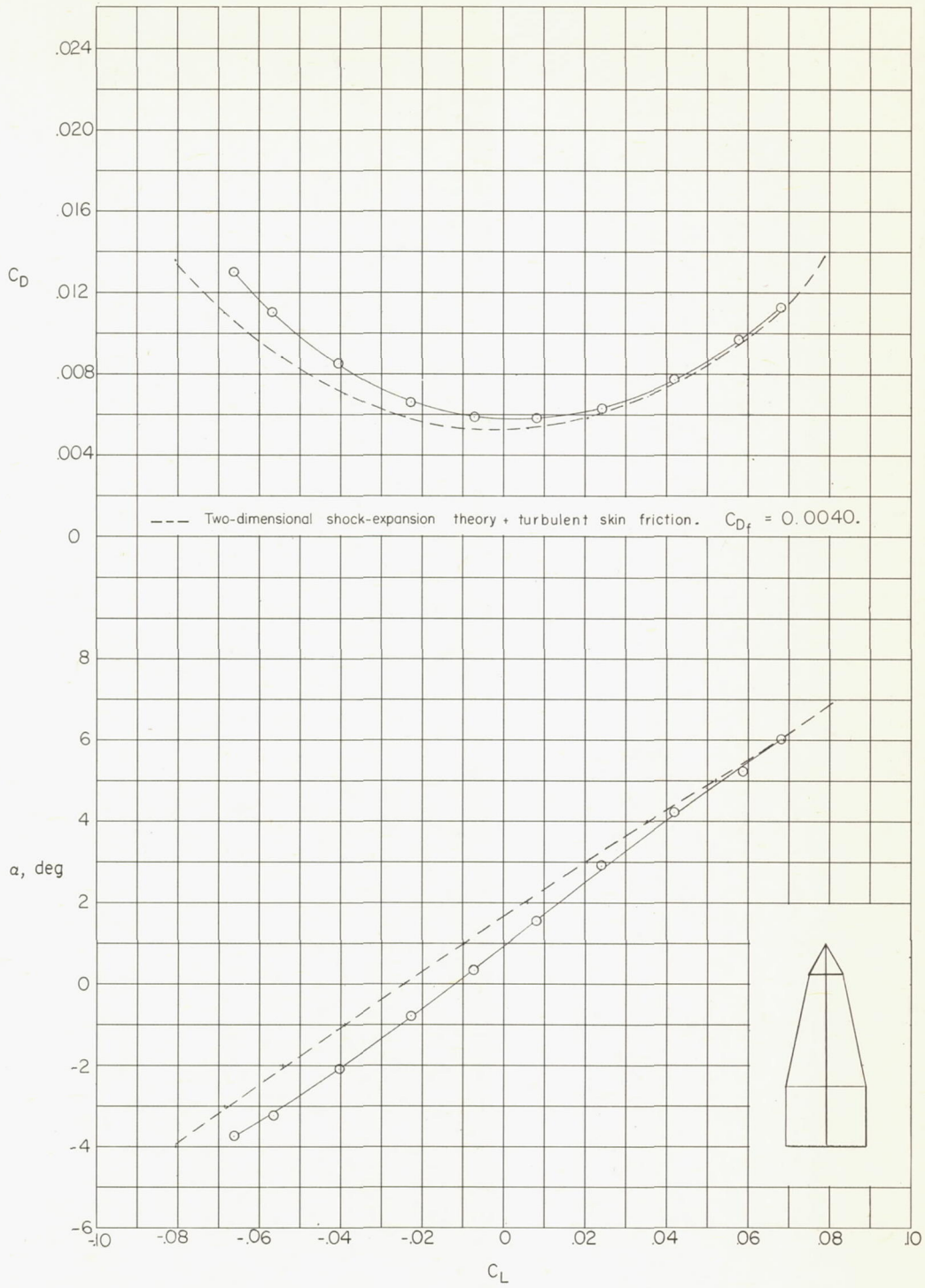

Figure 7.- Longitudinal aerodynamic characteristics of body 6 at M = 5.20.

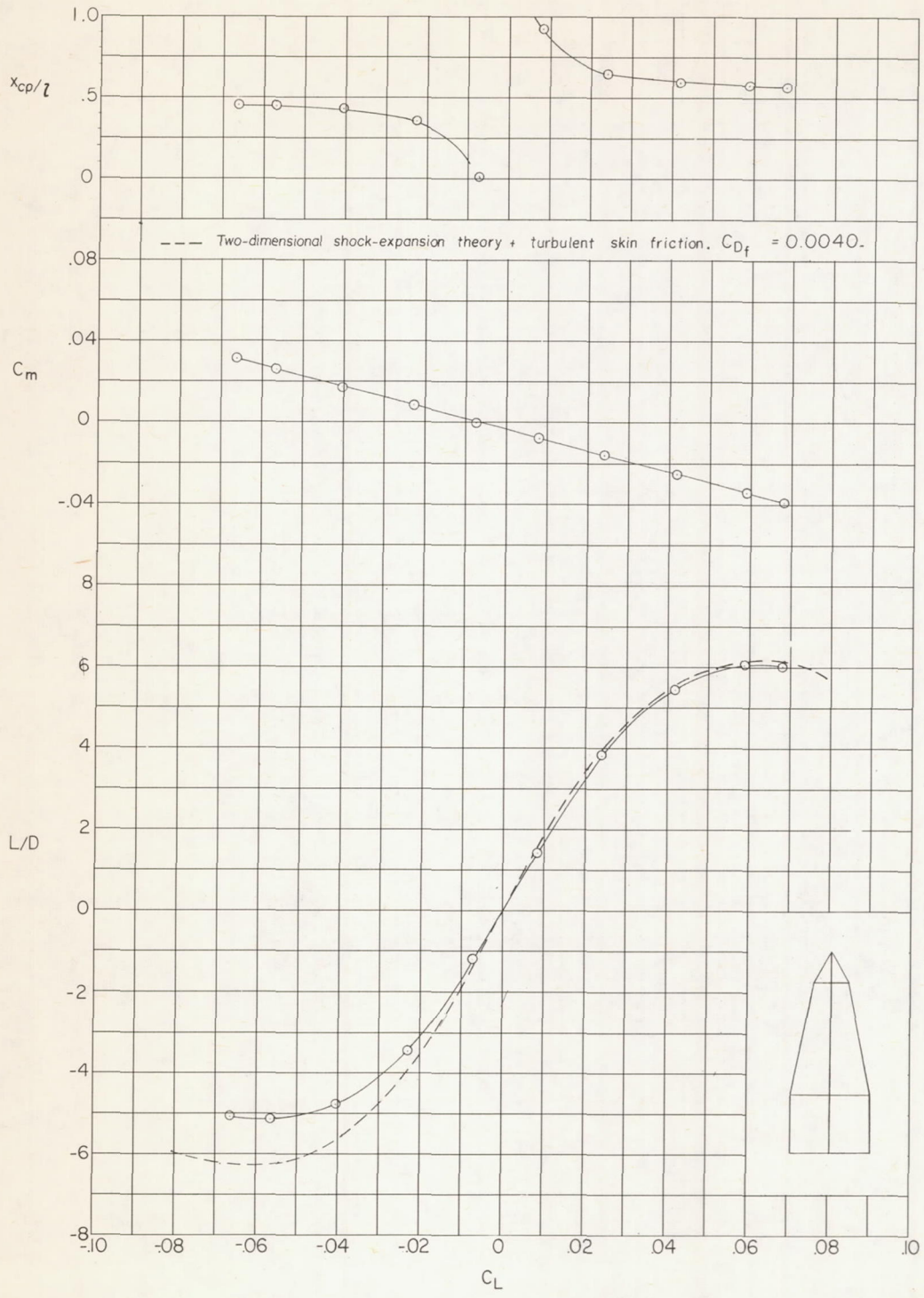

Figure 7.- Concluded.

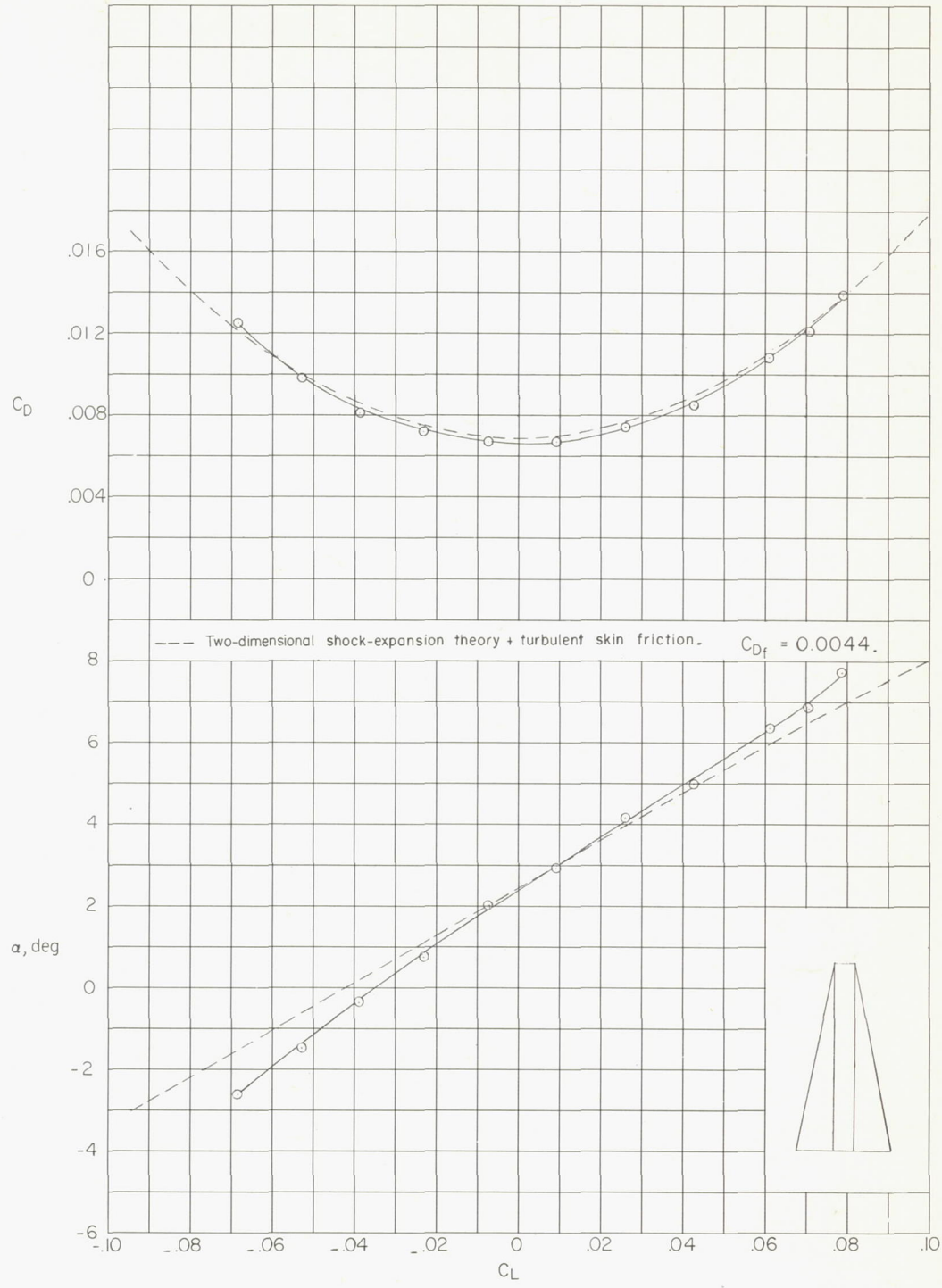

Figure 8.- Longitudinal aerodynamic characteristics of body 7 at M = 5.20.

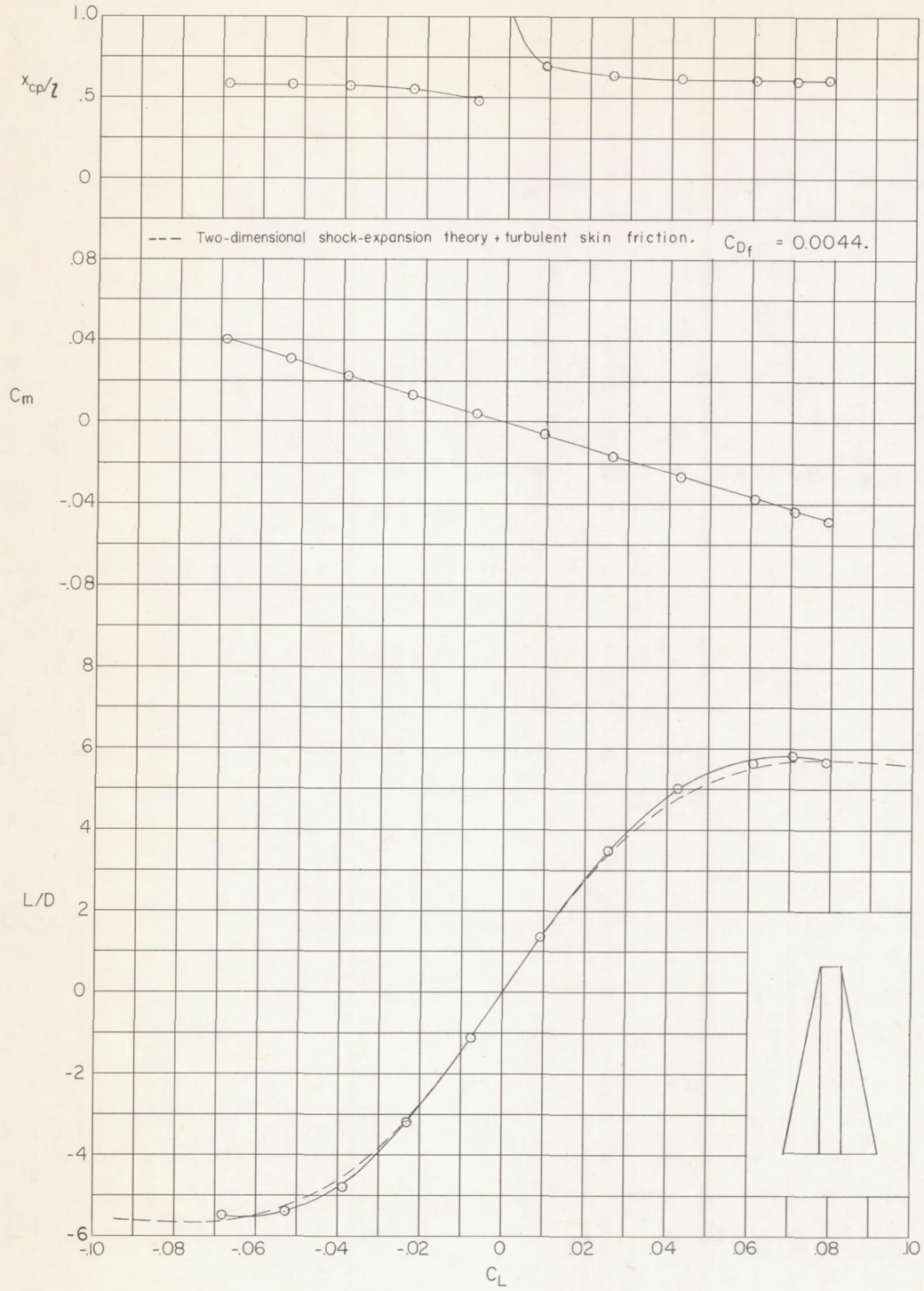

Figure 8.- Concluded.

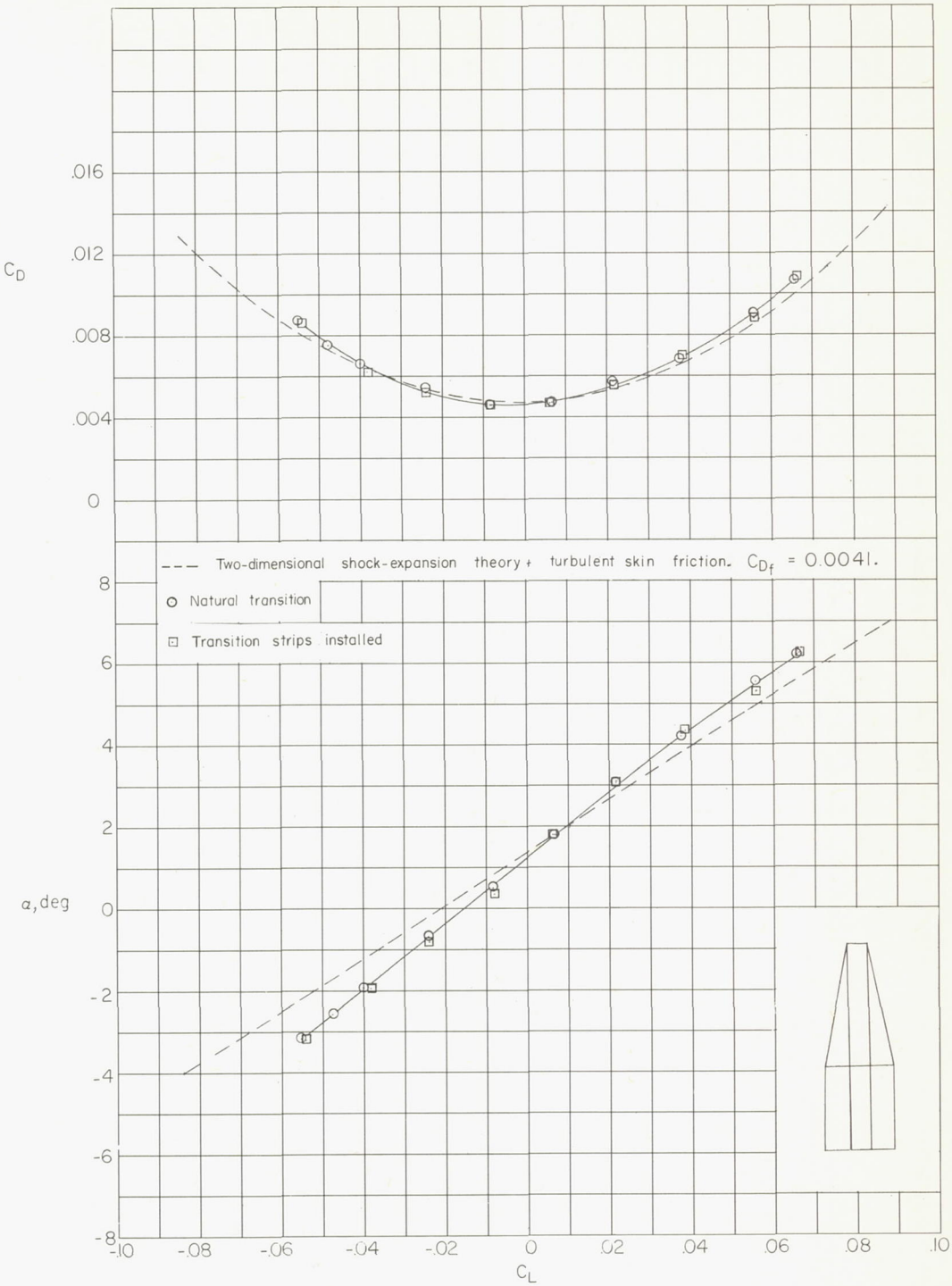

Figure 9.- Longitudinal aerodynamic characteristics of body 8 at M = 5.20.

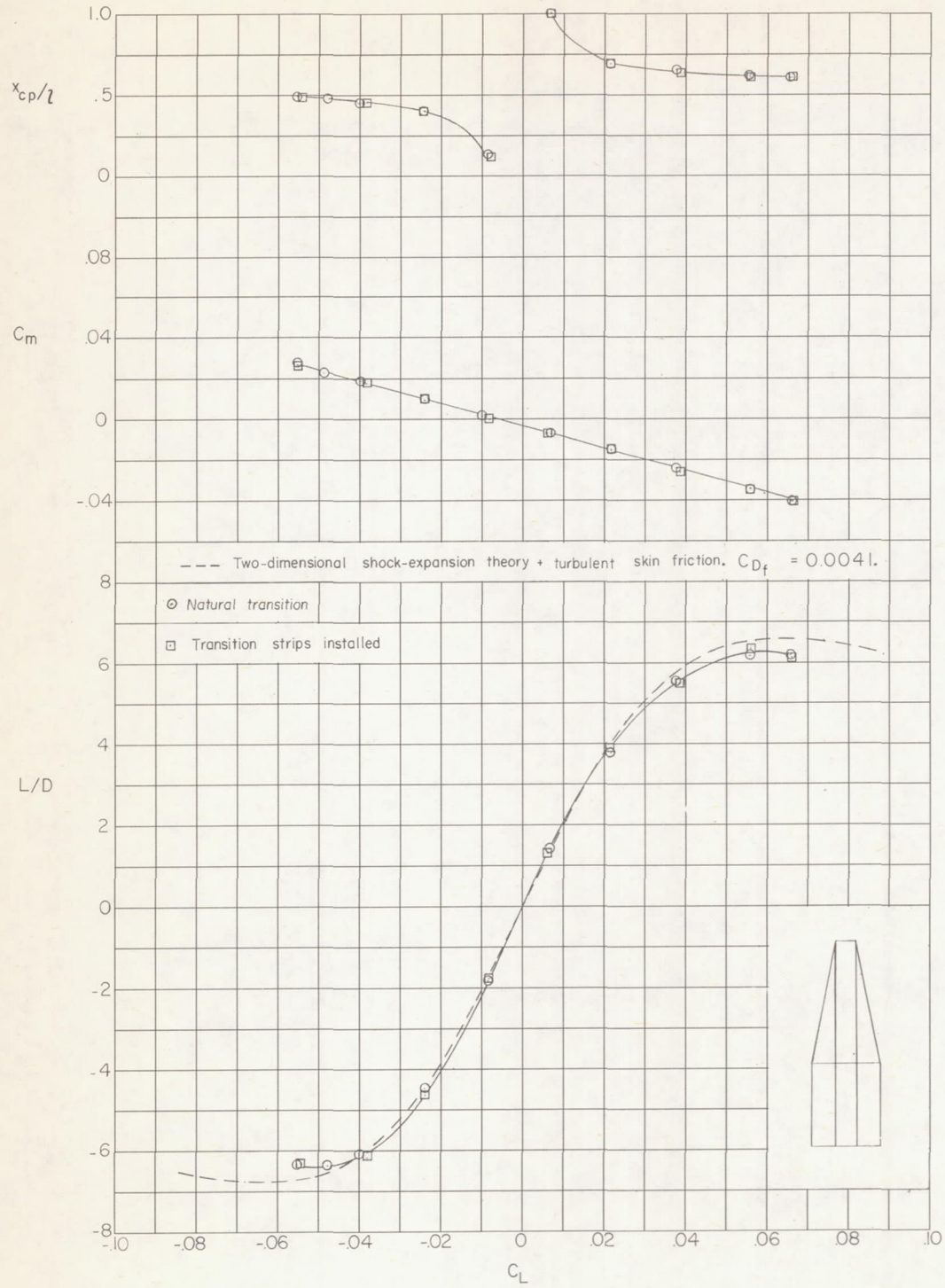

Figure 9.- Concluded.

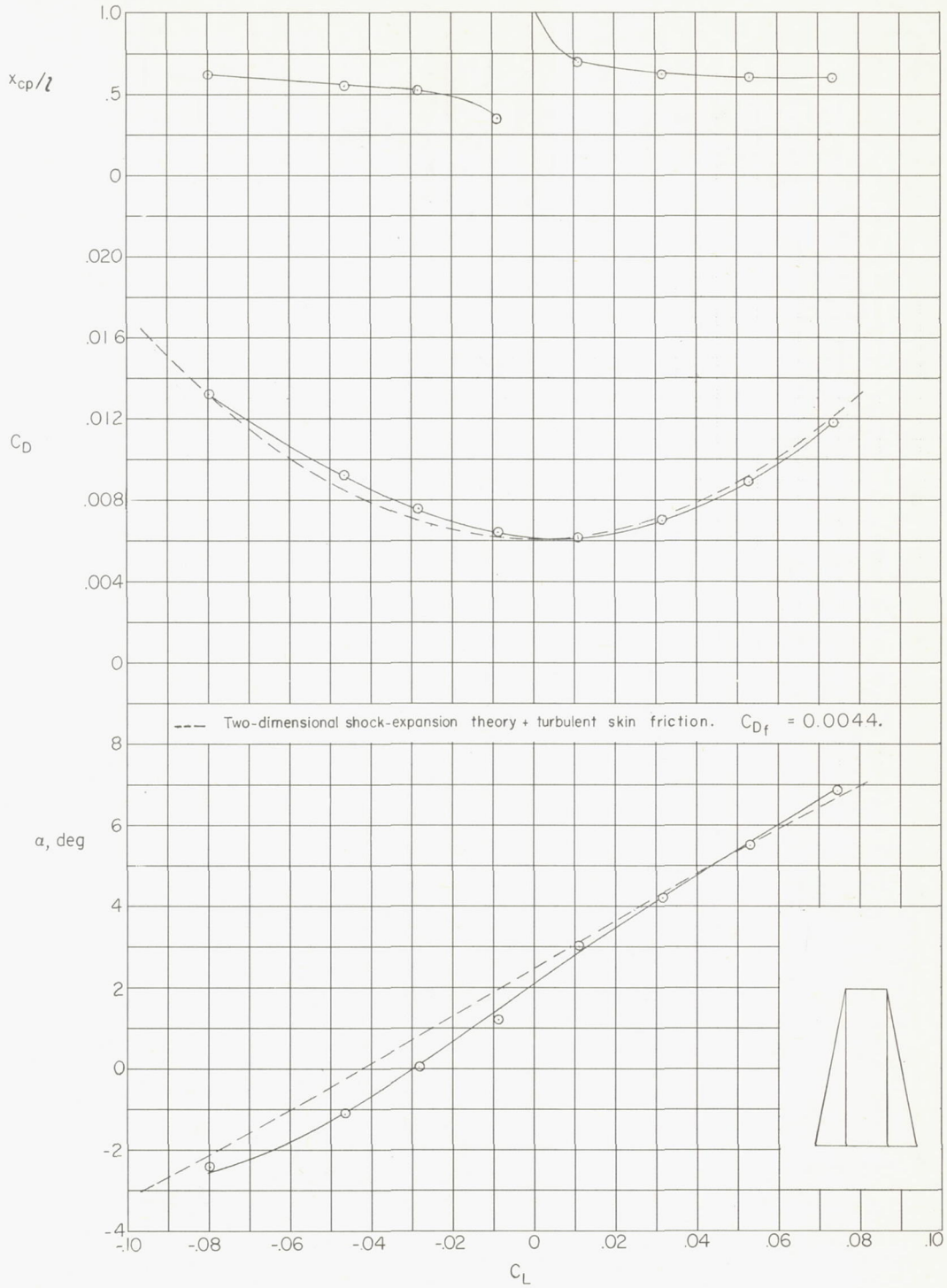

Figure 10.- Longitudinal aerodynamic characteristics of body 9 at M = 5.20.

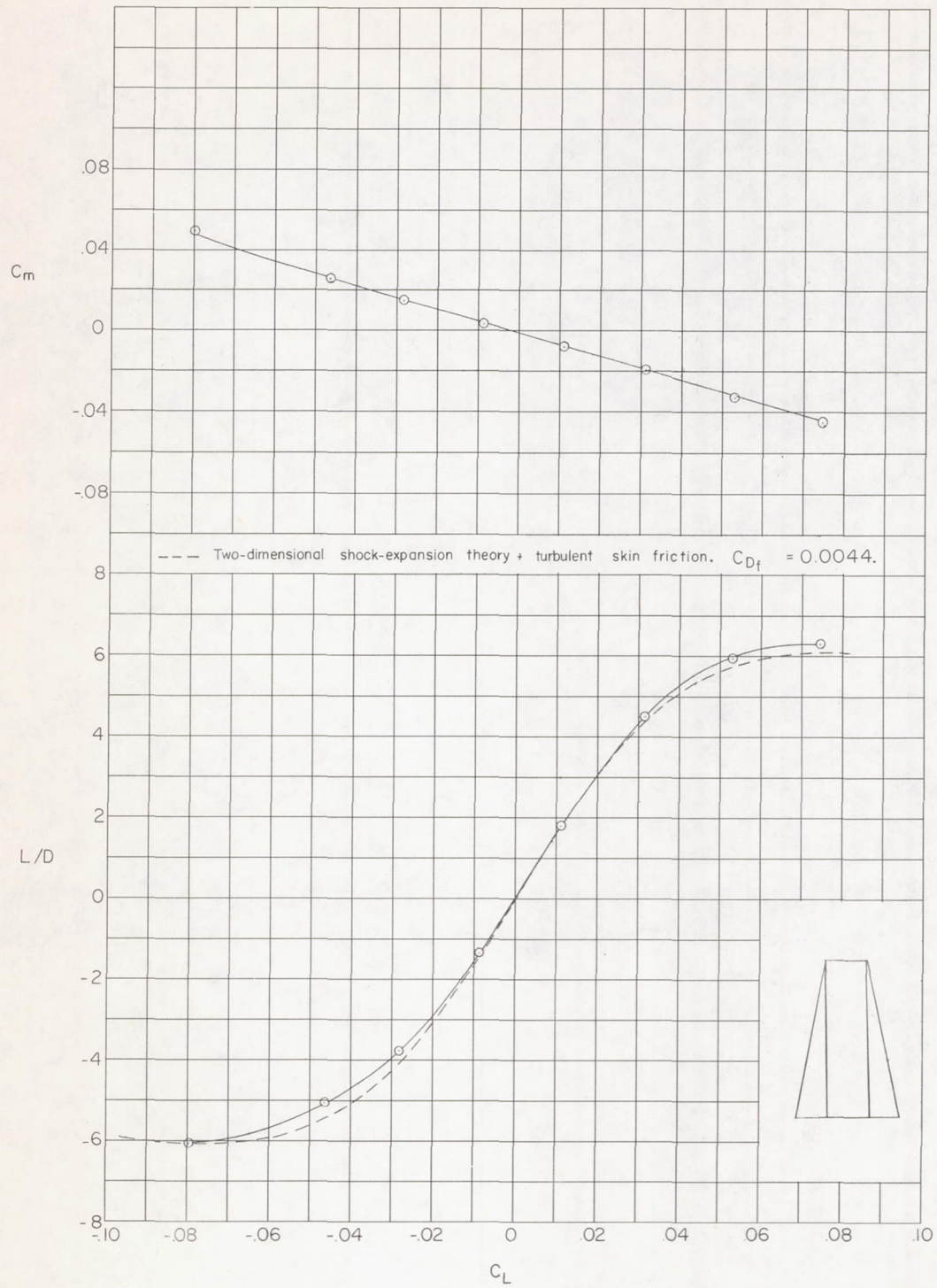

Figure 10.- Concluded.

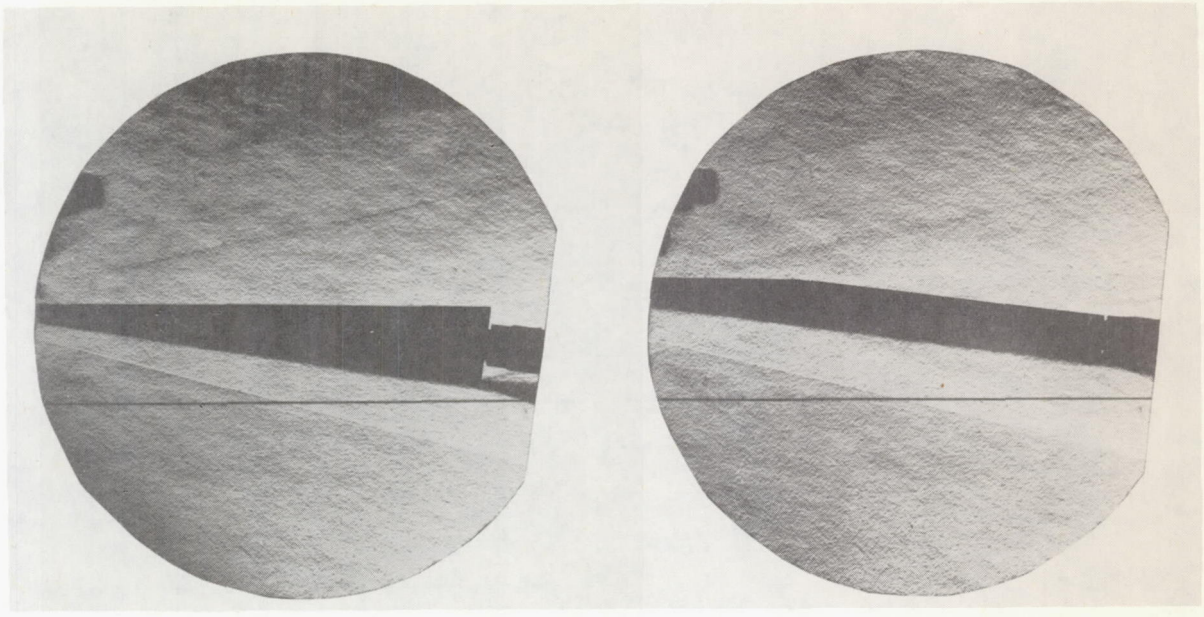

Body 1
α = 8.37°

Body 3
α = 6.95°

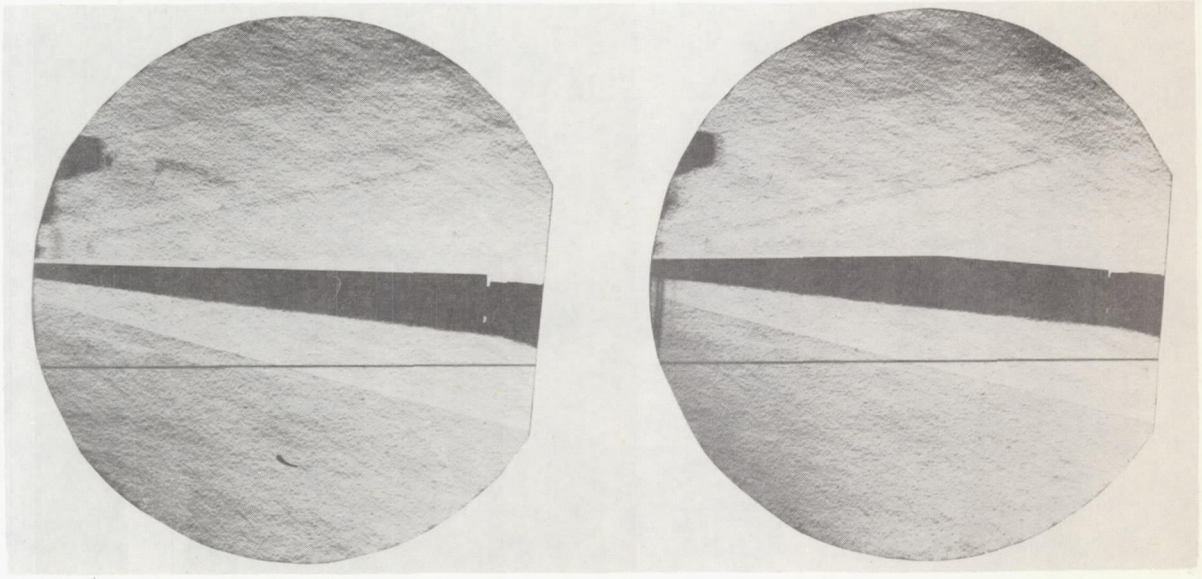

Body 4
α = 6.55°

Body 6
α = 5.23°

L-93521

Figure 11.- Schlieren photographs of four bodies at angles of attack for maximum lift-drag ratio.